The International Journal of Cardiovascular Imaging (2019) 35:937–945
https://doi.org/10.1007/s10554-018-01526-0

ORIGINAL PAPER

Image quality and radiation dose of two prospective ECG-triggered protocols using 128-slice dual-source CT angiography in infants with congenital heart disease

Baojin Chen[1] · Shuo Zhao[1] · Yang Gao[2] · Zhaoping Cheng[3] · Yanhua Duan[3] · Pritam Das[1] · Ximing Wang[1]

Received: 31 October 2018 / Accepted: 31 December 2018 / Published online: 17 January 2019

Abstract

This study aims to investigate the image quality and radiation dose of prospective ECG-triggered 128-slice dual-source CT (DSCT) angiography in the delineation of coronary arteries in infants with congenital heart disease (CHD). Sixty-three infants with CHD were randomly assigned into two groups: prospective ECG-triggered sequential protocol (group 1) and high-pitch spiral protocol (group 2). Patients were selected to the protocols randomly. A five-point scoring system was applied to study the capability of detecting coronary arteries. A score of <3 represents non-diagnostic. Effective radiation dose (ED) was calculated. The visualized rate for original, proximal, middle and distal segments of the coronary arteries was 98%, 95%, 94% and 83%, respectively in group 1, 93%, 82%, 53% and 34%, respectively in group 2. There were no significant demographic differences in the identification rate between the two groups as to the original and most of the proximal segments. Significant demographic differences were found in middle and distal segments ($p<0.05$). The mean ED of the high pitch group and the sequential group was 0.33 ± 0.11 mSv and 0.63 ± 0.16 mSv, respectively. Both the prospective ECG-gated high-pitch mode and the sequential mode for 128-slice DSCT allow satisfactory delineation of original and most of the proximal segments of coronary arteries in infants with CHD. However, an ECG-gated sequential mode is recommended when detailed anatomic assessment of the whole coronary arteries are needed since the ECG-gated high-pitch mode is limited in the delineation of middle and distal segments of the coronary arteries.

Keywords Coronary artery · Congenital heart disease · Infant · Prospective ECG-triggered 128-slice dual source computed tomography angiography

Introduction

The prevalence of congenital coronary artery anomalies (CAAs) is approximately 1.0% (0.3–2.2%) in the general population with structurally normal hearts [1]. Patients with congenital heart disease (CHD) have a higher incidence of CAAs than the general population [2]. Recognizing variability of CAAs is critical to prevent potential coronary artery related complications when considering surgical or interventional therapies in children with CHD [e.g. modification of tetralogy of Fallot (TOF), arterial switch operation or closure of coronary artery fistula (CAF)] [3, 4]. Postoperative evaluation of the coronary arteries is also important in the follow-up visit for that stenosis or occlusion may occur in some cases [5].

Recently, the rapid technical improvements in multidetector computed tomography have made it an effective tool for providing fast and accurate assessment for coronary

✉ Ximing Wang
xmwang369@126.com

1 Department of Radiology, Shandong Provincial Hospital, Key Laboratory of Diagnosis and Treatment of Cardio-cerebral Vascular Diseases, Shandong University, #324, Jingwu Road, Jinan 250021, Shandong, People's Republic of China

2 Department of Radiology, Fuwai Hospital, State Key Laboratory of Cardiovascular Disease, National Centre for Cardiovascular Diseases, Chinese Academy of Medical Sciences and Peking Union Medical College, #167 Bei-Li-Shi Street, Xi-Cheng District, Beijing 100037, People's Republic of China

3 Shandong Provincial Key Laboratory of Diagnosis and Treatment of Cardio-cerebral Vascular Diseases, Shandong Medical Imaging Research Institute, Shandong University, No.324, Jingwu Road, Jinan 250021, Shandong, People's Republic of China

arteries with excellent spatial resolution and anatomic coverage in children with CHD [6, 7]. With a high-pitch spiral mode provided by the second generation dual-source CT (DSCT), the proximal segments of the coronary arteries in children could be observed even without electrocardiography (ECG)-gating [8, 9]. However, a non-ECG-gated high-pitch spiral mode may be insufficient to provide preoperative information in patients who need a detailed evaluation of the anatomy of the coronary arteries. ECG-gating should be applied for a comprehensive assessment of coronary artery anatomy [8]. Retrospective ECG-triggered CT angiography is always associated with relatively high radiation dose and this remains the major limitation in its application in children [10]. Prospective ECG-triggered DSCT angiography including high-pitch spiral mode and the sequential scan mode was reported with relatively low radiation dose and was more commonly used in identifying coronary artery anatomy in children [7, 11]. However, visualization of the coronary arteries was found to be influenced by age and heart rate [12]. The performance of the two prospective ECG-triggered scan modes in the delineation of the coronary arteries has not been widely reported in infants. Thus, this randomized study aimed to assess the imaging quality of coronary arteries and radiation dose of the two prospective ECG-triggered scan modes with a 128-slice DSCT angiography in babies with CHD.

Materials and methods

Study design and patients

A total of 63 consecutive infants (37 male, 26 female) < 1-year-old (mean age 6.6 ± 3.7 months, 21 days to 1 year) with CHD underwent prospective ECG-triggered CT angiography between January 2017 and June 2018. CT angiography was performed to answer specific anatomical questions raised by inconclusive echocardiography before operation or for postoperative evaluation. Attention was paid to avoid administration of contrast material if contraindications existed, such as renal insufficiency, iodine intolerance or heart failure. The possible adverse effects of contrast medium and radiation exposure were explained to their legal guardians and informed consent forms were obtained in all patients. Study procedures were in accordance with the Declaration of Helsinki and the guidelines of the local ethics committee. The patients were randomly assigned into two groups: prospectively sequential acquisition (group 1) and high-pitch (3.4) spiral acquisition (group 2).

DSCT date acquisition

All CT examinations were performed with a 128-slice DSCT (Somatom Definition Flash; Siemens Healthcare, Forchheim, Germany). The scanning parameters were set as follows: 80 kV tuber voltage and weight adapted setting for tube current (60 mAs/rotation for patients < 5 kg body weight, 60–79 mAs/rotation for patients 5–10 kg body weight, 80–120 mAs/rotation for patients > 10 kg body weight), rotation time of 0.28 s; 2 × 64 × 0.6 mm detector collimation, a slice collimation 2 × 128 × 0.6 mm by z-flying focal spot technique. The start phase of CT data acquisition was at 45% of the R-R interval in group 1, and starting at 30% of R–R interval using a pitch of 3.4 in group 2. Patients were scanned in craniocaudal direction under a natural heart rate and quiet breathing after short-term sedation achieved with oral administration of chloral hydrate under the supervision of a pediatrician.

Iodinated contrast medium (Schering Ultravist, Iopromide, 350 mg I/ml, Berlin, Germany) was injected via peripheral vein by using a dual-head power injector. The volume was adjusted to the body weight: 1.2–1.5 ml/kg with a 10–20 ml saline chaser. Injection rate was calculated as 0.1 ml/s × body weight. Automatic bolus triggering software program was applied with a circular region of interest (ROI) positioned at the level of the descending aorta. When an attenuation threshold within the ROI exceeded 100 Hounsfield units (Hu), scan acquisition automatically commenced after a delay of 4–6 s.

Image post-processing and analysis

Images were reconstructed as follows: contiguous 0.75-mm thickness and increment of 0.4-mm using a medium smooth-tissue convolution kernel (I26f) with sinogram-affirmed iterative reconstruction (SAFIRE; Siemens Healthcare, Forchheim, Germany) strength 3. All images were transferred to an external workstation (Multiple Modality Workplace, Siemens Healthcare, Germany) for further analysis. In addition to the CT axial slices, multiple planar reconstruction, curved planar reformation, maximum intensity projection, and volume rendering were applied for image interpretation.

Each subject was analyzed independently by two cardiovascular radiologists with more than 10 years' experience. Both observers were blinded to the scanning parameters and patient characteristics. The coronary arteries were divided into 11 segments for evaluation including the origin of the left and right coronary artery (LCAo/RCAo), the main branch of left coronary artery (LCA) (LM), the proximal/middle/distal of the right coronary

artery (RCAp/RCAm/RCAd), the proximal/middle/distal of the left anterior descending artery (LADp/LADm/LADd) and the proximal/distal of the left circumflex artery (LCXp/LCXd) (Fig. 1). Each segment was assessed using a five-grade scale (Grade 5, clear visualization without any motion artifacts; Grade 4, mild motion artifacts, but still with high diagnostic confidence; Grade 3, obvious blurring; moderate diagnostic confidence; Grade 2, identified but equivocal, may simulate other structures; Grade 1, severe motion artifacts; no coronary segment visualized) [8]. In the segment of discordance between the two radiologists, the lower score was used. Scores of 3, 4, and 5 were considered sufficient diagnostic image quality.

To assess the image quality objectively, the average density of contrast media and standard deviation (SD) in Hu were measured in the root of ascending aorta on 0.75-mm thickness transverse slice. Attenuation was measured in the middle of the ascending aorta in a 1-cm^2 circular ROI. The noise was defined as the SD of the attenuation value, and the signal–noise ratio (SNR) was calculated as the ratio of the attenuation value and the noise.

Radiation dose estimations

The dose-length product (DLP) and the volume CT dose index (CTDIvol) were obtained from the information generated by the CT system. To calculate the effective dose (ED), the DLP was multiplied by a scanner-specific conversion factor provided by the manufacturer to adapt it to a 16-cm phantom: 2.3 for 80 kV. This value was then multiplied by the age-specific conversion coefficient for the chest: 0.039 mSv/[mGy cm] for children up to 4 months, 0.026 mSv/[mGy cm] between 4 months and 1 year of age [13].

Statistical analysis

Statistical analysis was performed with commercially available software (SPSS version 20.0, IBM Company, Chicago, IL). Continuous variables were expressed as mean ± SD (normal distribution) or median (interquartile range) (non-normal distribution). Categorical variables were expressed as frequencies or percentages. Interobserver agreement on grades of image quality score was assessed by kappa statistics ($\kappa = 0.41$–0.60, moderate agreement; $\kappa = 0.61$–0.80, good agreement; $\kappa > 0.81$, excellent agreement) [14]. Categorical variables were compared using the Chi-squared test. Continuous variables that were normally distributed were compared by independent samples t-test. Mann–Whitney U test was used in the comparison of continuous variables that were not normally distributed. Value of $p < 0.05$ was considered statistically significant.

Results

Population characteristics

The final diagnosis of 63 patients were TOF with other abnormalities (n = 34), coarctation of aorta with other abnormalities (n = 7), double aortic arch (n = 1), aortopulmonary window (n = 3), pulmonary atresia (n = 3), pulmonary artery sling (n = 1), anomalous pulmonary venous drainage (n = 5), double outlet right ventricle (n = 3), transposition of the great arteries (n = 2), post-operation of Blalock–Taussig shunt (n = 2), and CAA (n = 2). Finally, four cases were found to have CCAs. Three in the sequential group and one in the high-pitch group. In the sequential group, one was TOF with right coronary artery (RCA) originating from the left coronary sinus, one

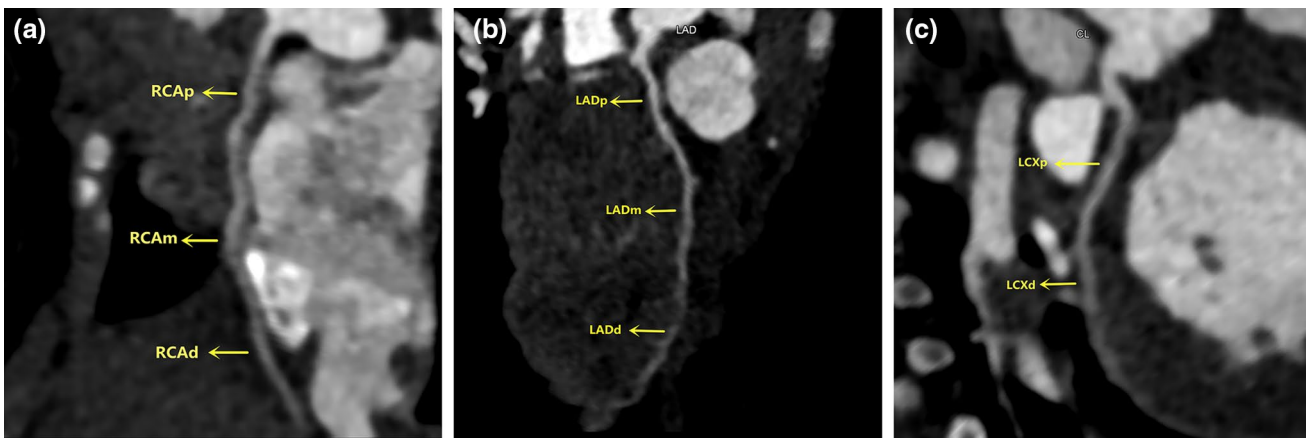

Fig. 1 Segments of coronary arteries were denoted on the CT images. *RCAp/RCAm/RCAd* proximal/middle/distal of the right coronary artery, *LADp/LADm/LADd* proximal/middle/distal of the left anterior descending artery, *LCXp/LCXd* proximal/distal of the left circumflex artery

was RCA right ventricular fistulae (Fig. 2), and one was LCA originating from pulmonary artery (Fig. 3). All the three CCAs have been confirmed during surgery. In the high-pitch group, the patient was coarctation of aorta with RCA originating from the left coronary sinus (Fig. 4). The average weight was 6.9 ± 2.1 kg (range 3–11.5 kg). The mean heart rate was 121.0 ± 16.2 beats per minute (bpm) (range 95–162 bpm). Patient characteristics are presented in Table 1. There was no significant difference in gender, age, weight, and heart-beats between the two groups (all $p > 0.05$).

Subjective assessment of the image quality

Interobserver agreement of the coronary image quality was reached in 645 (93.1%) segments (Kappa = 0.903). Disagreement occurred in 48 segments and all of them had only one point of difference. The mean scores of the two groups in accessing the 11 segments of coronary arteries are illustrated in Table 2. There was no statistical difference in the original segments, RCAp, and LM between the two groups. The mean scores of LADp and LCXp were lower in group 2. The visualized rate (score ≥ 3) of the 11 segments of coronary arteries are illustrated in Table 3. Visualized rate in group 1 and group 2 was 98% (65/66) and 93% (56/60) for the

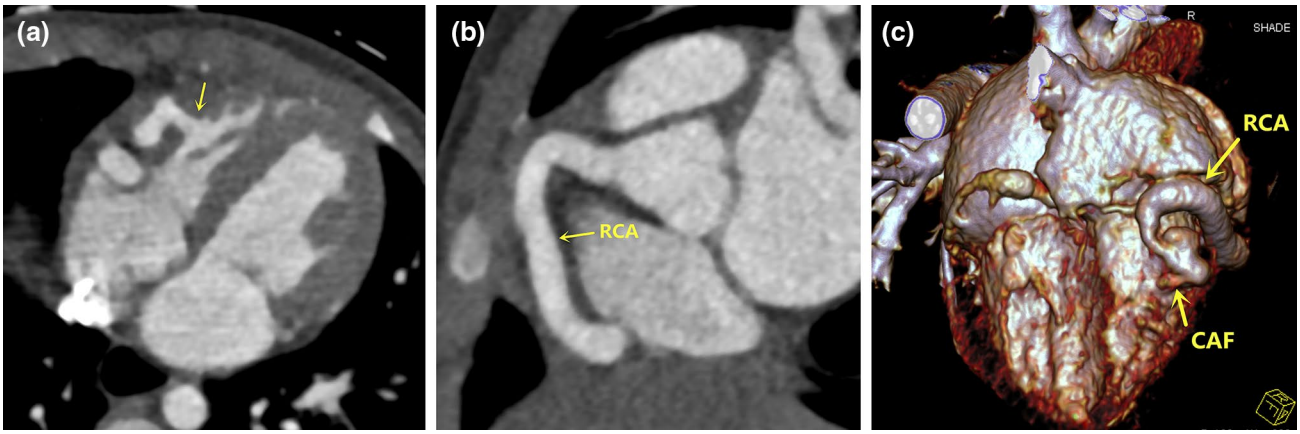

Fig. 2 A 4-month-old girl suspected to have CAF underwent CT angiography with an ECG-gated sequential mode. **a** The axial image shows the fistula from the RCA to the right ventricle (arrow). **b** Multiple planar reconstruction shows the dilated RCA. **c** Volume rendering demonstrates the distal aneurysmal and tortuous RCA and the CAF

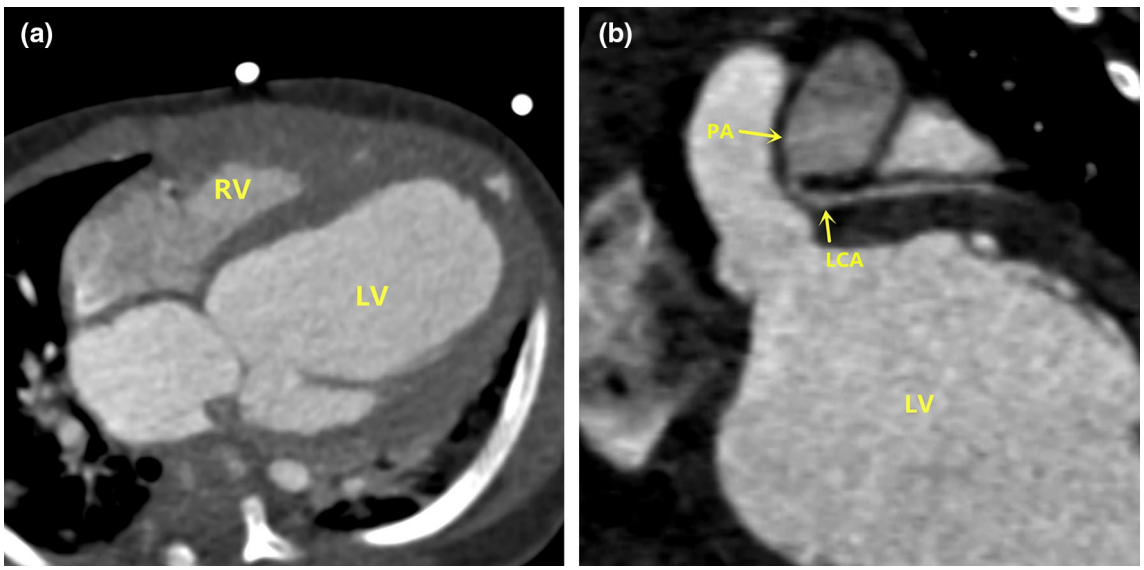

Fig. 3 A 3-month-old boy suffering from lung infections was suspected to have anomalous origin of LCA by ultrasonography. **a** The axial image shows the dilated left ventricle (LV) and the normal right ventricle (RV). **b** Maximum intensity projection demonstrates the anomalous origin of LCA from pulmonary artery (PA)

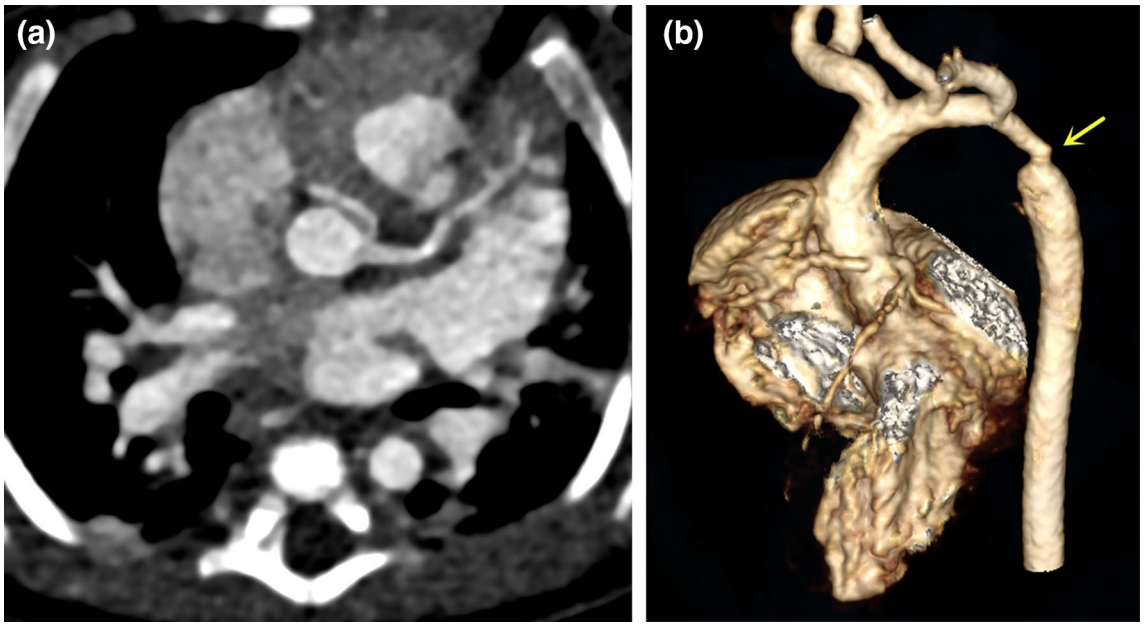

Fig. 4 A 6-week-old boy suspected to have aortic coarctation underwent CT angiography with an ECG-gated high-pitch mode. **a** Multiple planar reconstruction shows the RCA originated from the left coronary sinus; **b** volume rendering demonstrates the original and the proximal segments of coronary arteries and the aortic coarctation (arrow)

Table 1 Patient characteristics and scanning protocols

Groups	N (male)	Scan mode	Age (months)	Weight (kg)	Heart rate (bpm)
Group 1	33 (20)	Sequential	6.5 ± 3.5	7.1 ± 2.2	123.4 ± 17.4
Group 2	30 (17)	High-pitch	6.8 ± 4.0	6.7 ± 2.0	118.2 ± 14.6
p-value	0.751		0.738	0.454	0.207
In total	63 (37)		6.6 ± 3.7	6.9 ± 2.1	121.0 ± 16.2

Table 2 Subjective image quality evaluation of sequential protocol and high-pitch protocol

Segment	In total	Sequential	High-pitch	*p*-Value
RCAo	4.46 ± 0.93	4.48 ± 0.80	4.43 ± 1.07	0.658
LCAo	4.46 ± 0.86	4.64 ± 0.60	4.27 ± 1.05	0.179
RCAp	4.10 ± 1.24	4.33 ± 0.96	3.83 ± 1.46	0.199
LM	4.54 ± 0.90	4.76 ± 0.50	4.30 ± 1.15	0.107
LADp	4.10 ± 1.15	4.52 ± 0.83	3.63 ± 1.27	0.002
LCXp	3.30 ± 1.24	3.82 ± 1.24	2.73 ± 0.98	< 0.001
RCAm	3.60 ± 1.43	4.18 ± 1.07	2.97 ± 1.52	0.001
LADm	3.54 ± 1.52	4.30 ± 1.07	2.70 ± 1.57	< 0.001
RCAd	3.13 ± 1.57	3.97 ± 1.36	2.43 ± 1.61	0.001
LADd	3.13 ± 1.60	3.97 ± 1.36	2.20 ± 1.32	< 0.001
LCXd	2.71 ± 1.47	3.45 ± 1.30	1.9 ± 1.21	< 0.001

LCAo/RCAo origin of the left and right coronary artery, *LM* the main branch of left coronary artery, *RCAp/RCAm/RCAd* proximal/middle/distal of the right coronary artery, *LADp/LADm/LADd* proximal/middle/distal of the left anterior descending artery, *LCXp/LCXd* proximal/distal of the left circumflex artery

original segments, 94% (31/33) and 83% (25/30) for RCAp, 100% (33/33) and 93% (28/30) for LM, 97% (32/33) and 86% (26/30) for LADp, respectively. There were no significant differences in the identification rate between two groups as to original and most of the proximal segments ($p > 0.05$). Significant differences were found in other six segments (RCAm, RCAd, LADm, LADd, LCXp, and LCXd) for the visualized rate ($p < 0.05$).

Objective evaluation of image quality

The average attenuation, average noise, and the average SNR in the root of ascending aorta were 430.2 ± 89.1 Hu, 18.3 ± 6.1 Hu and 25.5 ± 7.8, respectively by the sequential group and 455.0 ± 78.8 Hu, 19.1 ± 3.3 Hu and 24.2 ± 4.1, respectively by the high-pitch group. There was no significant difference in average attenuation, average noise, and the average SNR between the sequential group and high-pitch group (all $p > 0.05$).

Table 3 Visibility of coronary arteries of sequential protocol and high-pitch protocol

Segment	In total, count (%)		Sequential, count (%)		High-pitch, count (%)		*p*-Value
	Score ≥ 3	Score < 3	Score ≥ 3	Score < 3	Score ≥ 3	Score < 3	
Original segments	121 (96)	5 (4)	65 (98)	1 (2)	56 (93)	4 (7)	0.139
RCAo	60 (95)	3 (5)	32 (97)	1 (3)	28 (93)	2 (7)	0.498
LCAo	61 (97)	2 (3)	33 (100)	0 (0)	28 (93)	2 (7)	0.132
Proximal segments	223 (88)	29 (12)	125 (95)	7 (5)	98 (82)	22 (18)	0.001
RCAp	56 (89)	7 (11)	31 (94)	2 (6)	25 (83)	5 (17)	0.181
LM	61 (97)	2 (3)	33 (100)	0 (0)	28 (93)	2 (7)	0.132
LADp	58 (92)	5 (8)	32 (97)	1 (3)	26 (86)	4 (14)	0.131
LCXp	48 (76)	15 (24)	29 (88)	4 (12)	19 (63)	11 (37)	0.022
Middle segments	94 (75)	32 (25)	62 (94)	4 (6)	32 (53)	28 (47)	< 0.001
RCAm	48 (76)	15 (24)	31 (94)	2 (6)	17 (57)	13 (43)	0.001
LADm	46 (73)	17 (27)	31 (94)	2 (6)	15 (50)	15 (50)	< 0.001
Distal segments	113 (60)	76 (40)	82 (83)	17 (17)	31 (34)	59 (66)	< 0.001
RCAd	41 (65)	22 (35)	28 (85)	5 (15)	13 (43)	17 (57)	0.001
LADd	39 (62)	24 (38)	29 (88)	4 (12)	10 (33)	20 (67)	< 0.001
LCXd	33 (52)	30 (48)	25 (76)	8 (24)	8 (26)	22 (74)	< 0.001

There were no significant differences in the identification rate between two groups as to original and most of the proximal segments ($p > 0.05$)

Radiation dose estimation

The radiation dose parameters are summarized in Table 4. Significant differences were found in CTDIvol, DLP and ED between the high-pitch group and the sequential group (all $p < 0.05$) (Fig. 5). The mean ED of the high pitch group and the sequential group was 0.33 ± 0.11 mSv and 0.63 ± 0.16 mSv, respectively. The high-pitch group had a 48% reduction compared with the sequential group.

Discussion

In the present study, we investigated the image quality and radiation dose of two prospective ECG-triggered protocols using 128-slice DSCT in the delineation of coronary arteries in infants with CHD. Both the high-pitch spiral acquisition and the sequential acquisition made a satisfactory delineation of the original and most of the proximal segments (except for LCXp) of the coronary arteries. The imaging quality of LCXp, middle segments and the distal segments of the coronary arteries was inferior in the high-pitch group compared with the sequential group. As to the radiation dose, the high-pitch group had a 48% reduction compared with the sequential group.

Presurgical identification of some CCAs is clinically important because the presence of the anomaly results in modification of the surgical technique. For example, any major coronary artery branch crossing the right ventricular outflow tract may result in a modification of the surgical technique in a surgical correction of TOF. Recently, the rapid developments in multi-detector CT have made it an important tool in the assessment of coronary arteries in pediatric patients with CHD [6, 7, 15]. Goo and Yang [16] reported that 97.1% of the original and 71.9% of the proximal segments were traceable with a prospective ECG-triggered sequential scanning. Ben Saad et al. [17] reported that 91% of the LCA and 84% of the RCA had a diagnostic image quality in the proximal segments with a retrospective ECG-triggered spiral scanning. In our study, the sequential group also provided a satisfactory delineation in original (98%), proximal (95%), middle (94%) and the distal (83%)

Table 4 Radiation dose of the two groups

Groups	CTDI (mGy)			DLP (mGy/cm)			ED (mSv)		
	25%	50%	75%	25%	50%	75%	25%	50%	75%
Group 1	0.73	0.95	1.19	8.00	10.00	12	0.50	0.63	0.72
Group 2	0.29	0.33	0.39	5.00	6.00	6.00	0.25	0.30	0.42
In total	0.32	0.63	1.00	5.00	7.00	10.00	0.30	0.50	0.63

Significant differences were found in CTDIvol, DLP and ED between the two groups, all $p < 0.001$

group 1 = sequential group, group 2 = high-pitch group

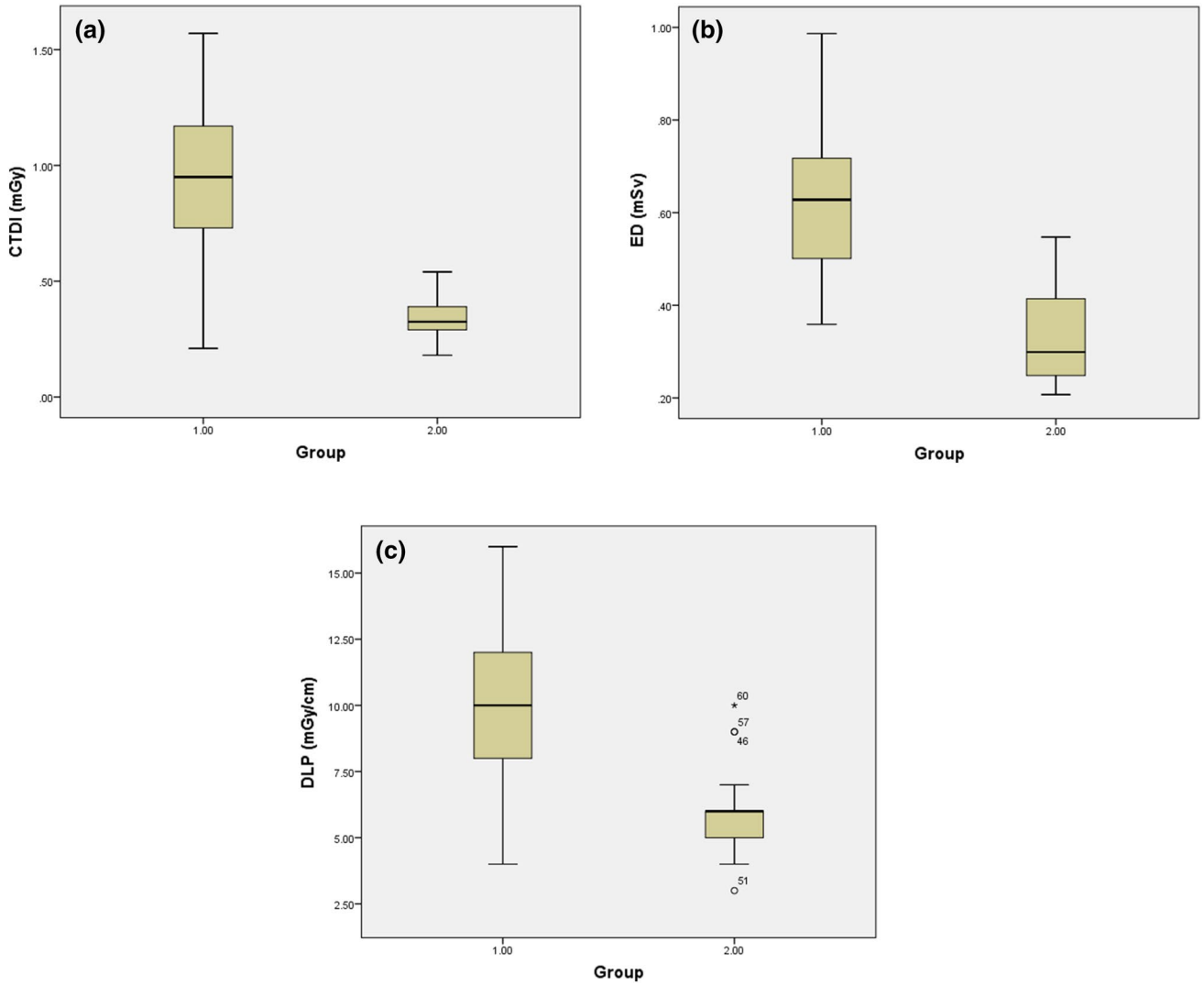

Fig. 5 DLP, volume CT dose index (CTDIvol) and ED of the two groups (group 1 = sequential group, group 2 = high-pitch group, significant difference was found in every radiation dose index between the two groups, all $p < 0.001$)

segments. Li et al. [11] reported that 80% of the coronary artery was traceable with a prospective ECG-triggered high-pitch scanning. However, the image quality for which segment was not specified in their study. In our cohort, the high-pitch group made a satisfactory delineation in original (93%) and the proximal (82%) segments. However, the visualized rate of LCXp was inferior in the high-pitch group compared with the sequential group. This may be attributed to the small size of LCXp. The visualized rate in the middle (53%) and distal (34%) segments was significantly lower compared with the original and proximal segments. It may be insufficient in the delineation of middle and distal segments of coronary arteries in infants using a second generation DSCT scanner.

The second generation DSCT system provided a high-pitch spiral scanning mode. With a flash table speed of 460 mm/s and a high pitch of 3.4, the entire volumetric data could be acquired in one single cardiac cycle [18]. Kanie et al. [8] reported that 80.5% of the proximal segments of coronary arteries had diagnostic image quality in a high-pitch spiral scanning mode even without an ECG-gating. However, in our study, high-pitch spiral scanning was insufficient in the delineation of middle and distal segments of coronary arteries even with an ECG-gating. This may be attributed to that images acquired with this scan mode show different cardiac phases along the z-axis [19]. Besides, heart rates of infants are always high and unstable. Data acquisition was either too early or too late in the cardiac cycle when the heart rates were irregular [13]. Hence, the sequential mode was recommended for these patients who suspected to have middle or distal anomalies

such as CAF or TOF with major coronary artery branch crossing the right ventricular outflow.

Radiation safety has always been a great concern for pediatric patients. A significant cumulative dose may lead to acute radiation-induced chromosomal DNA damage in children with CHD [20]. Therefore, we must choose optimal protocol to decrease radiation dose as low as reasonably achievable, while meeting demand for the diagnostic task. In our protocol design, a retrospectively spiral acquisition was not included because it always referred to a high radiation dose [11, 17, 21]. With a sequential scanning, we got a 0.63 mSv in our study after correction for body size. In the high-pitch spiral scanning group, ED had a 48% reduction compared with the sequential group. So a high-pitch protocol could be used to lower the radiation dose for these patients who have no CCAs or only suspected to have anomalies in original segments.

Our study was unique in several aspects. First, our study was a prospective randomized design. Infants with CHD were assigned to use sequential and high-pitch spiral protocol randomly regardless of his or her age, weight or heart rate. Second, the patients enrolled in this study were infants. The performance in the coronary arteries delineation of the high-pitch spiral protocol with a 128-slice DSCT had not been evaluated in infants. Third, we performed an assessment on the image quality of the middle and distal segments of the coronary arteries in addition to the original and proximal segments.

There are several limitations to our study. Firstly, retrospective ECG-gating spiral scan protocol and non-ECG-gating high-pitch spiral scan protocol were not included in our study because the two protocols was not widely used in clinical practice in our hospital. Secondly, our study is mainly based on a subjective scoring system for image quality. The diagnostic accuracy compared with conventional angiography or surgery findings should be investigated in the future.

In conclusion, both the prospective ECG-gated high-pitch mode and the sequential mode for 128-slice DSCT allow satisfactory delineation of original and most of the proximal segments of coronary artery in infants with CHD. However, an ECG-gated sequential mode is recommended when detailed anatomic assessment of the whole coronary arteries are needed since the ECG-gated high-pitch mode is limited in the delineation of middle and distal segments of the coronary arteries.

Funding This study has received funding by National Natural Science Foundation of China Grant Nos. 81371548 (X. Wang) and 81571672 (X. Wang) and a Taishan Scholar Projection (X. Wang).

Compliance with ethical standards

Conflict of interest The authors of this manuscript declare no relationships with any companies, whose products or services may be related to the subject matter of the article.

Ethical approval This study was approved by the Institutional Review Board and written informed consent was obtained from the parents/guardians of all participants.

Research involving human participants and/or animals All applicable international, national, and/or institutional guidelines for the care and use of animals were followed.

References

1. Goo HW, Seo DM, Yun TJ, Park JJ, Park IS, Ko JK, Kim YH (2009) Coronary artery anomalies and clinically important anatomy in patients with congenital heart disease: multislice CT findings. Pediatr Radiol 39(3):265–273
2. Yu FF, Lu B, Gao Y, Hou ZH, Schoepf UJ, Spearman JV, Cao HL, Sun ML, Jiang SL (2013) Congenital anomalies of coronary arteries in complex congenital heart disease: diagnosis and analysis with dual-source CT. J Cardiovasc Comput Tomogr 7(6):383–390
3. Lowry AW, Olabiyi OO, Adachi I, Moodie DS, Knudson JD (2013) Coronary artery anatomy in congenital heart disease. Congenit Heart Dis 8(3):187–202
4. Zhang Q, Duan Y, Hongxin L, Wenbin G (2017) An innovative technique of perventricular device closure of a coronary artery fistula through a left parasternal approach. Eur Heart J 38(42):3177
5. Angeli E, Formigari R, Pace Napoleone C, Oppido G, Ragni L, Picchio FM, Gargiulo G (2010) Long-term coronary artery outcome after arterial switch operation for transposition of the great arteries. Eur J Cardio-thorac Surg 38(6):714–720
6. Yao LP, Zhang L, Li HM, Ding M, Yu LW, Yang X, Li XM, Sun K (2017) Assessment of coronary artery by prospective ECG-triggered 256 multi-slice CT on children with congenital heart disease. Int J Cardiovasc Imaging 33(12):2021–2028
7. Goo HW (2018) Identification of coronary artery anatomy on dual-source cardiac computed tomography before arterial switch operation in newborns and young infants: comparison with transthoracic echocardiography. Pediatr Radiol 48(2):176–185
8. Kanie Y, Sato S, Tada A, Kanazawa S (2017) Image quality of coronary arteries on non-electrocardiography-gated high-pitch dual-source computed tomography in children with congenital heart disease. Pediatr Cardiol 38(7):1393–1399
9. Han BK, Lindberg J, Grant K, Schwartz RS, Lesser JR (2011) Accuracy and safety of high pitch computed tomography imaging in young children with complex congenital heart disease. Am J Cardiol 107(10):1541–1546
10. Goo HW (2010) State-of-the-art CT imaging techniques for congenital heart disease. Korean J Radiol 11(1):4–18
11. Li T, Zhao S, Liu J, Yang L, Huang Z, Li J, Luo C, Li X (2017) Feasibility of high-pitch spiral dual-source CT angiography in children with complex congenital heart disease compared to retrospective-gated spiral acquisition. Clin Radiol 72(10):864–870
12. Young C, Taylor AM, Owens CM (2011) Paediatric cardiac computed tomography: a review of imaging techniques and radiation dose consideration. Eur Radiol 21(3):518–529
13. Nie P, Wang X, Cheng Z, Ji X, Duan Y, Chen J (2012) Accuracy, image quality and radiation dose comparison of high-pitch spiral and sequential acquisition on 128-slice dual-source CT angiography in children with congenital heart disease. Eur Radiol 22(10):2057–2066
14. Landis JR, Koch GG (1977) The measurement of observer agreement for categorical data. Biometrics 33(1):159–174
15. Cheng Z, Wang X, Duan Y, Wu L, Wu D, Chao B, Liu C, Xu Z, Li H, Liang F, Xu J, Chen J (2010) Low-dose prospective ECG-triggering dual-source CT angiography in infants and children with

complex congenital heart disease: first experience. Eur Radiol 20(10):2503–2511
16. Goo HW, Yang DH (2010) Coronary artery visibility in free-breathing young children with congenital heart disease on cardiac 64-slice CT: dual-source ECG-triggered sequential scan vs. single-source non-ECG-synchronized spiral scan. Pediatr Radiol 40(10):1670–1680
17. Ben Saad M, Rohnean A, Sigal-Cinqualbre A, Adler G, Paul JF (2009) Evaluation of image quality and radiation dose of thoracic and coronary dual-source CT in 110 infants with congenital heart disease. Pediatr Radiol 39(7):668–676
18. Esser M, Gatidis S, Teufel M, Ketelsen I, Nikolaou K, Schafer JF, Tsiflikas I (2017) Contrast-enhanced high-pitch computed tomography in pediatric patients without electrocardiography triggering and sedation: comparison of cardiac image quality with conventional multidetector computed tomography. J Comput Assist Tomogr 41(1):165–171
19. Goo HW (2015) Coronary artery imaging in children. Korean J Radiol 16(2):239–250
20. Ait-Ali L, Andreassi MG, Foffa I, Spadoni I, Vano E, Picano E (2010) Cumulative patient effective dose and acute radiation-induced chromosomal DNA damage in children with congenital heart disease. Heart 96(4):269–274
21. Lee T, Tsai IC, Fu YC, Jan SL, Wang CC, Chang Y, Chen MC (2006) Using multidetector-row CT in neonates with complex congenital heart disease to replace diagnostic cardiac catheterization for anatomical investigation: initial experiences in technical and clinical feasibility. Pediatr Radiol 36(12):1273–1282